

A Primer on the Statistical Relation between Wireless Ultra-Reliability and Location Estimation

Tobias Kallehauge, Pablo Ramírez-Espinosa, Kimmo Kansanen, Henk Wymeersch *Senior Member, IEEE*, and Petar Popovski, *Fellow, IEEE*

Abstract—This letter statistically characterizes the impact of location estimation uncertainty in the wireless communication reliability, in which location information is used as a proxy to choose the rate. First, a Cramér-Rao bound for the localization error is derived. Then, through a simplified setup, we show that the reliability — characterized by how likely the outage probability is to be above a target threshold — can be sensitive to location errors, especially when the channel statistics are also sensitive to the location. Finally, we highlight the difficulty of choosing a rate that both meets target reliability and accounts for the location uncertainty, and that the most direct solutions suffer from being too conservative.

I. INTRODUCTION

User localization and ultra-reliable low-latency communications (URLLC) are ubiquitous concepts in 5G networks [1]. Reliability of wireless transmission is related — among others — to the behavior of the propagation channel and the interference, and propagation and interference statistics are inherently correlated with spatial location. Consequently, exploiting this relation is envisioned as a promising direction in mobile networks, e.g., using location information to assist millimeter-wave communications [2], the generation of channel maps for increased reliability and predictive resource allocation [3]–[5], and channel charting for user localization [6]. The standardization by 3rd Generation Partnership Project (3GPP) of minimization of drive tests (MDT) [7] is an additional motivation, allowing the operators to take advantage of end-user devices measurements for the previously mentioned tasks.

In contrast to more conventional approaches where samples are acquired over time to estimate channel statistics and thus reliability [8], the relation between channel and location brings forward the idea of using location to infer channel statistics and, ultimately, as a proxy for guaranteeing reliability in URLLC. Considering the latency introduced by estimating channel statistics, a communication system that predicts reliability based on location using only a few measurements, is an attractive alternative. However, these reliability-guaranteeing methods would rely, among other aspects, on the ability to estimate location accurately, which raises the question: *How*

can the accuracy of the localization procedures impact the wireless reliability guarantees?

In this letter, we address for the first time the previous question by considering a simplified but illustrative one-dimensional scenario, where a user equipment (UE) is intended to communicate with a base station (BS), and the rate is selected based *only* on the estimated location. The localization performance is characterized through Fisher information analysis [9], and reliability is statistically characterized following the meta-probability approach in [8]. To isolate the impact of location uncertainty, we assume that the UE location completely determines the channel statistics and that this mapping is known. Even for this very simple scenario we show that location errors lead to non-negligible changes in the communication reliability, especially when the channel statistics rapidly varies with the location. Also, it is highlighted that choosing the transmission rate satisfying a target statistical criterion is a non-trivial task.

Notation: $\Re(z)$ and $\Im(z)$ are the real and imaginary parts of a complex number z , and j is the imaginary unit. $(\cdot)^T$ and $(\cdot)^H$ are the matrix transpose and conjugate transpose, and $\|\cdot\|$ is the ℓ_2 norm. For matrix \mathbf{A} , the submatrix with row i to j and column k to p is denoted $\mathbf{A}_{i:j,k:p}$. $\mathcal{N}(\mu, \sigma^2)$ and $\mathcal{CN}(\mu, \sigma^2)$ denote Gaussian and complex circular symmetric Gaussian distributions with mean μ and variance σ^2 . Finally, $E[\cdot]$ and $\text{Var}[\cdot]$ denote, respectively, the expectation and the variance operators.

II. SYSTEM MODEL

A. Communication system and channel model

We consider a simple 1D framework with two BSs at locations $x_1, x_2 \in \mathbb{R}$ which communicate with a UE at location $x \in \mathbb{R}$. For simplicity, both BSs and the user are equipped with a single antenna. An orthogonal frequency division multiplexing (OFDM) modulation scheme is considered, with bandwidth W and N subcarriers spaced $\Delta_f = W/N$.

The channel between the UE and the BS $i \in \{1, 2\}$ is assumed to be time-independent, and it follows a two-path model. Thus, the baseband equivalent impulse response is given by

$$h_i(\tau) = \sqrt{P_{\text{tx}}} \sum_{k=1}^2 a_{i,k} \delta(\tau - \tau_{i,k}), \quad (1)$$

where P_{tx} is the transmit power, $a_{i,k}$ is the complex channel coefficient for path k and $\delta(\cdot)$ is the Dirac delta function. The first path ($k = 1$) characterizes the line-of-sight (LoS) link,

This work was partially supported by the Villum Investigator Grant in Denmark.

T. Kallehauge, P. Ramírez-Espinosa and P. Popovski are with the Department of Electronic Systems, Aalborg University, Denmark (e-mail: tkal@es.aau.dk; pres@es.aau.dk; petarp@es.aau.dk).

K. Kansanen is with the Norwegian University of Science and Technology, Trondheim, Norway (e-mail: kimmo.kansanen@ntnu.no).

H. Wymeersch is with Chalmers University of Technology, Gothenburg, Sweden (e-mail: henkw@chalmers.se).

TABLE I
SYSTEM SETTINGS.

Symbol	Description	Value
$[x_1, x_2]$	BS locations	$[0, 1000]$ m
P_{tx}	Transmit power pr. sub-carrier	10 dBm
σ_n^2	Noise variance	-70 dBm
W	Bandwidth	10 MHz
f_c	Center frequency	2.1 GHz
N	Number of sub-carriers	600
$\Delta\tau_i$	Excess delay (same for $i = 1, 2$)	50 ns
ρ	Parameter for power delay profile	2

being therefore deterministic and geometrically-dependent as [10], [11]

$$a_{i,1} = \sqrt{\frac{\lambda^2}{16\pi^2 d_i^2}} e^{-j2\pi d_i/\lambda} = \sqrt{P_L(d_i)} e^{-j\phi(d_i)}, \quad (2)$$

where λ is the wavelength and $d_i = \|x - x_i\|$. Naturally, it follows that $\tau_{i,1} = \|x - x_i\|/c$ with c the speed of light. The second path ($k = 2$) represents the contribution of the scattered paths, which cannot be mutually resolved and hence $a_{i,2} \sim \mathcal{CN}(0, \sigma_i^2(\Delta\tau_i))$ with variance according to an exponential power delay profile [12]:

$$\text{Var}[a_{i,2}] = \sigma_i^2(\Delta\tau_i) = \frac{P_{L,i}}{\rho} \exp\left(-\frac{\Delta\tau_i}{\rho}\right), \quad (3)$$

where $\Delta\tau_i = \tau_{i,2} - \tau_{i,1}$ is the excess delay and $\rho > 0$ controls how fast the power fades as a function of $\Delta\tau_i$. Note that the choice to model $a_{i,2}$ statistically, unlike, e.g., the deterministic geometric models in [11], is made to allow for statistical analysis of the communication reliability.

Given a modulated signal block $\mathbf{s} \in \mathbb{C}^N$, the received baseband signal in the frequency domain from BS i across the different subcarriers, $\tilde{\mathbf{y}}_i \in \mathbb{C}^N$, is given by¹ [11]

$$\tilde{\mathbf{y}}_{i,j} = \sqrt{P_{\text{tx}}}\tilde{h}_{i,j}s_j + \tilde{n}_{i,j} \quad (4)$$

for $j = 0, \dots, N-1$, where $\tilde{n}_{i,j} \sim \mathcal{CN}(0, \sigma_n^2)$ is the noise term with variance σ_n^2 , $\tilde{h}_{i,j} = a_{i,1}d_j(\tau_{i,1}) + a_{i,2}d_j(\tau_{i,2})$ is the Fourier transform of (1) and $d_j(\tau) = \exp(-j\pi 2j\Delta_f\tau)$. The system settings used in the examples throughout this letter are summarized in Table I. Note that some of the values are chosen to produce results that clearly show the effect of location uncertainty on reliability with less emphasis on modeling a realistic scenario.

B. Localization and communication protocol

The following simple (albeit illustrative) two-step protocol is assumed:

1) When the UE turns on for the first time, it estimates its location using a ping — a single OFDM signal block as in (4) with $s_j = 1 \forall j$ — from each BS. To that end, time of arrival (TOA) estimation is employed. Moreover, the pings are used to select the BS with which the UE will communicate based on the received power, i.e., BS $i \in \{1, 2\}$ is chosen such that $\|\tilde{\mathbf{y}}_i\|^2$ is maximized.

2) Once the UE has estimated its location and the target BS, it starts the communication with the chosen BS by sending

information symbols (power normalized $E[|s_j|^2] = 1$) through different OFDM blocks at a rate R . To isolate the impact of the location uncertainty in the reliability, we assume that the channel distribution is completely determined by the location, i.e., given a location x , the user knows the distribution of $\tilde{h}_{i,j} \forall i, j$. Hence, from the estimated position \hat{x} , the UE selects a constant rate to communicate with the chosen BS.

III. STATISTICS OF LOCALIZATION AND COMMUNICATION

A. Localization

In TOA localization, location is estimated based on the propagation delay of the LoS path, although the accuracy of this method suffers when the UE and BS clocks are not perfectly synchronized [13]. Time difference of arrival (TDOA) localization can be used to cancel the clock bias [13], but for the sake of simplicity in the statistical analysis, we use TOA and introduce the effect of clock bias B in the localization uncertainty, i.e., the measured delay is $\tilde{\tau}_{i,1} = \|x - x_i\|/c + B$. Given the received signals $\tilde{\mathbf{y}}_1, \tilde{\mathbf{y}}_2$ from (4), we use the Cramér-Rao inequality to characterize the variance of any unbiased estimator of x as

$$\text{Var}[\hat{x}(\tilde{\mathbf{y}}_1, \tilde{\mathbf{y}}_2)] \geq J^{-1}(x), \quad (5)$$

where $J^{-1}(x)$ is the Fisher information corresponding to the location x [14]. To find $J(x)$, we first derive the Fisher information with respect to the unknown parameters

$$\boldsymbol{\eta}_i = [\tilde{\tau}_{i,1} \quad \tilde{\tau}_{i,2} \quad \Re(a_{i,1}) \quad \Im(a_{i,1}) \quad \Re(a_{i,2}) \quad \Im(a_{i,2})]^\top \quad (6)$$

for $i = 1, 2$. For fixed channel coefficients, the normalized received signal $\tilde{\mathbf{y}}_i/\sqrt{P_{\text{tx}}}$ follows a circular symmetric, complex Gaussian distribution with mean $\boldsymbol{\mu}(\boldsymbol{\eta}_i) = a_{i,1}\mathbf{d}(\tilde{\tau}_{i,1}) + a_{i,2}\mathbf{d}(\tilde{\tau}_{i,2})$ and covariance $\frac{\sigma_n^2}{P_{\text{tx}}}\mathbf{I}_{N \times N}$. Therefore [14]:

$$J(\boldsymbol{\eta}_i) = \frac{2P_{\text{tx}}}{\sigma_n^2} \sum_{j=0}^{N-1} \Re \left(\frac{\partial \mu_j}{\partial \boldsymbol{\eta}_i} \left(\frac{\partial \mu_j}{\partial \boldsymbol{\eta}_i} \right)^H \right), \quad (7)$$

whose closed form expression is omitted here due to space limitation. In $\boldsymbol{\eta}_i$, the LoS delay $\tilde{\tau}_{i,1}$ contains information about the location x , so we continue with the equivalent Fisher information [9]

$$J^E(\tilde{\tau}_i) = J(\boldsymbol{\eta}_i)_{1,1} - J(\boldsymbol{\eta}_i)_{1,2:6} J^{-1}(\boldsymbol{\eta}_i)_{2:6,2:6} J(\boldsymbol{\eta}_i)_{2:6,1} \quad (8)$$

where the second term is interpreted as the information loss from the unknown variables. Due to independence of the TOA signals, $J^E(\tilde{\tau}_{1,1}, \tilde{\tau}_{2,1})$ is the diagonal matrix with entries $J^E(\tilde{\tau}_{1,1}), J^E(\tilde{\tau}_{2,1})$ and the Fisher information with respect to (x, B) is obtained using the transformation [14]

$$J(x, B) = \mathbf{T}^\top J^E(\tilde{\tau}_{1,1}, \tilde{\tau}_{2,1}) \mathbf{T}, \quad \mathbf{T} = \begin{bmatrix} \frac{\partial \tilde{\tau}_{1,1}}{\partial x} & \frac{\partial \tilde{\tau}_{1,1}}{\partial B} \\ \frac{\partial \tilde{\tau}_{2,1}}{\partial x} & \frac{\partial \tilde{\tau}_{2,1}}{\partial B} \end{bmatrix}. \quad (9)$$

Finally, $J^{-1}(x) = (J(x, B)^{-1})_{1,1}$ gives the Cramér-Rao lower bound, which is assumed for the variance of \hat{x} . Additionally, we assume the asymptotic result in which the location estimator \hat{x} follows a Gaussian distribution [15], that is $\hat{x} \sim \mathcal{N}(x, J^{-1}(x))$. The variance $J^{-1}(x)$ contains the random channel coefficients from the scatter paths, $a_{1,2}, a_{2,2}$, and it turns out that only the phases of these, $\phi_{1,2}, \phi_{2,2}$,

¹We assume identical uplink and downlink channels.

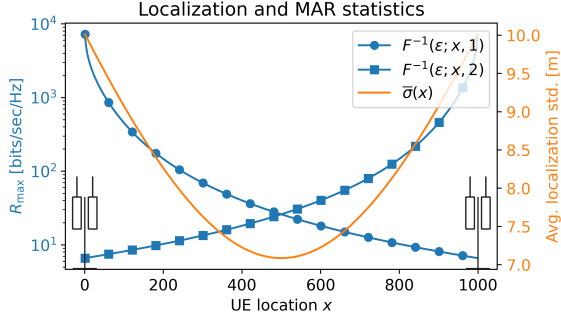


Fig. 1. Statistics for localization and MAR. The inverse CDF $F^{-1}(\epsilon; x, i)$ is the ϵ -quantile for R_{\max} at location x when communicating with BS i . Here, $\epsilon = 10^{-3}$, $\bar{\sigma}^2(x)$ is the localization variance $\sigma^2(x; \phi)$ averaged over ϕ ; the figure shows the standard variation $\bar{\sigma}(x)$.

affect the variance while the magnitudes cancel. Denoting $\sigma^2(x; \phi) = J^{-1}(x)$ and using that $\phi = [\phi_{1,2} \ \phi_{2,2}]^T$ is uniform on $[0, 2\pi)^2$, we get the hierarchical model for the output of the localization algorithm

$$\hat{x} | \phi \sim \mathcal{N}(x, \sigma^2(x; \phi)), \quad \phi \sim \text{uniform}([0, 2\pi)^2). \quad (10)$$

For the sake of illustration, Fig. 1 shows localization uncertainty for different locations x .

B. Rate and Communication Reliability

At the physical layer, we assess the system's reliability by its ability to choose a communication rate R that does not exceed the maximum achievable rate (MAR) R_{\max} . In our case, from (4), the instantaneous MAR for the channel between the UE at location x and BS i is given by [10]

$$R_{\max}(x, i) = \sum_{j=0}^{N-1} \log_2 \left(1 + \frac{|\tilde{h}_{i,j}|^2}{N_0} \right). \quad (11)$$

Fig. 1 shows statistics for R_{\max} as a function of location x . Reliability is characterized by the outage probability

$$P(R > R_{\max}(x, i)) = F(R; x, i), \quad (12)$$

where $F(\cdot)$ is the cumulative distribution function (CDF) for R_{\max} . When propagation statistics are known, target reliability of $\epsilon > 0$ is achieved by selecting a rate $R = F^{-1}(\epsilon; x, i)$. However, if F is not perfectly known, the selected rate does not meet the outage requirement, and the concept of meta-probability and probably correct reliability arise [8].

Here, as stated in Sec. II-B, it is assumed that the CDF has been mapped for all locations prior to transmission, i.e., given a location x , $F^{-1}(\epsilon; x, i)$ is perfectly known. Therefore, after estimating its location \hat{x} , the UE selects the rate using some function $R_{\epsilon, i}(\hat{x})$ (specific examples are introduced in Sec. IV). Note that, since the CDF is assumed known given x , this scenario represents an upper bound in the performance of location-based rate selection methods. However, even in this idealized scenario, we will see that location uncertainty can severely affect the reliability and throughput of the transmission if the rate is not selected carefully.

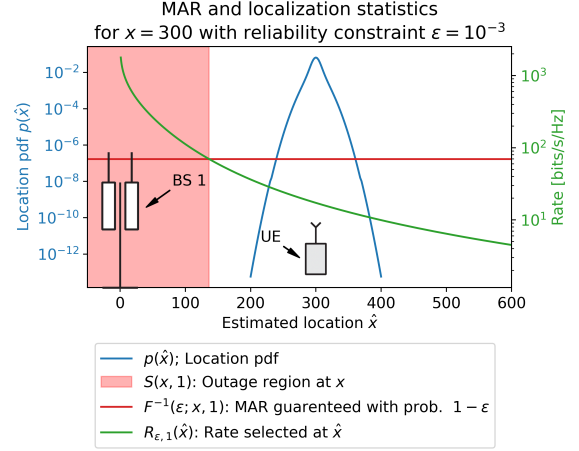


Fig. 2. Meta-probability statistics with backoff rate selection function $R_{\epsilon, i}(\hat{x}) = 0.25 \cdot F^{-1}(\epsilon; \hat{x}, i)$ (see Sec. IV-A). The location probability density function (PDF) $p(\hat{x})$ is the marginal PDF of $p(\hat{x}, \phi)$ according to (10) obtained through numerical integration. The UE location is 300 m while the outage region is $[-136.2, 136.2]$ m.

To evaluate reliability, we resort to outage probability and meta-probability as in [8]. Hence, given an estimated location \hat{x} , the outage probability is given by

$$\begin{aligned} p_{\text{out}}(x, \hat{x}; i) &= P(R_{\epsilon, i}(\hat{x}) > R_{\max}(x, i) | \hat{x}, i) \\ &= F(R_{\epsilon, i}(\hat{x}); x, i), \end{aligned} \quad (13)$$

and the meta-probability for the link between the UE and BS i is [8, Eq. (15)]

$$\begin{aligned} \tilde{p}_{\epsilon}(x; i) &= P(P(R_{\epsilon, i}(\hat{x}) > R_{\max}(x, i) | \hat{x}, i) > \epsilon) \\ &= P_{\hat{x}}(p_{\text{out}}(x, \hat{x}; i) > \epsilon). \end{aligned} \quad (14)$$

Assuming block fading where $R_{\max}(x, i)$ is drawn independently for each block, (14) gives the probability that any of these blocks violates the reliability constraint ϵ . Averaging over the BSs we have

$$\tilde{p}_{\epsilon}(x) = \sum_{i=1}^2 P_{\hat{x}}(p_{\text{out}}(x, \hat{x}; i) > \epsilon) p_i(i; x), \quad (15)$$

where $p_i(i; x)$ is the probability of selecting BS i which is obtained through Monte-Carlo simulation according to Sec. II-B². In (15), the first factor is rewritten by introducing the *outage region*

$$S(x, i) = \{\hat{x} \in \mathbb{R} | p_{\text{out}}(x, \hat{x}; i) > \epsilon\} \quad (16)$$

such that

$$P_{\hat{x}}(p_{\text{out}}(x, \hat{x}; i) > \epsilon) = P_{\hat{x}}(\hat{x} \in S(x, i)). \quad (17)$$

The outage region is interpreted as the region of estimated locations \hat{x} where the rate selection function chooses a rate that is too optimistic for the MAR at location x . Fig. 2 depicts various statistics relevant for the meta-probability using one of the rate selection functions from Sec. IV. It is observed that the UE will choose an overly optimistic rate if it thinks it is closer to the BS than it actually is. The particular rate selection

²The estimated location \hat{x} and selected BS i are dependent since they use the same signal, but their dependence is neglected for the reliability analysis.

function shown in Fig. 2 is somewhat conservative; therefore, the outage region is pushed away from the UE, and the meta-probability is the probability mass from localization inside the outage region.

Together with the meta-probability, the other metric we use to evaluate location-based rate selection methods is the throughput ratio, defined as the ratio [8]

$$\omega_\epsilon(x) = \frac{E[R_{\epsilon,i}(\hat{x}) \mathbb{1}\{R_{\epsilon,i}(\hat{x}) \leq R_{\max}(x,i)\}]}{E[R_{\epsilon,i}^*(x) \mathbb{1}\{R_{\epsilon,i}^*(x) \leq R_{\max}(x,i)\}]}, \quad (18)$$

between the throughput using $R_{\epsilon,i}(\hat{x})$ and the optimal throughput using $R_{\epsilon,i}^*(x) = F^{-1}(\epsilon; x, i)$ where $\mathbb{1}$ the indicator function. The throughput is generally difficult to analyze, but for the class of rate selection functions used in Sec. IV, it fulfills $\omega_\epsilon(x) < 1$ given a reliability constraint, i.e., an upper bound for $\tilde{p}_\epsilon(x)$. Some of the functions have the additional property that $\omega_\epsilon(x) \rightarrow 1$ for $\text{Var}[\hat{x}] \rightarrow 0^3$.

The throughput ratio is expanded with repeated use of the law of total expectation, yielding

$$\omega_\epsilon(x) = \frac{E_i[E_\phi[E_{\hat{x}|\phi}[R_{\epsilon,i}(\hat{x})(1 - p_{\text{out}}(x, \hat{x}; i)) | i, \phi] | i]]}{E_i[R_{\epsilon,i}^*(x)(1 - \epsilon)}. \quad (19)$$

IV. LOCATION-AWARE RATE SELECTION

Location-based rate selection methods naturally depends on the rate function $R_{\epsilon,i}(\hat{x})$, and the ultimate goal would be to solve the optimization problem

$$\sup_{R_{\epsilon,i}} \int \omega_\epsilon(x) dx, \quad \text{s.t.} \quad \tilde{p}_\epsilon(x) \leq \delta \quad \forall x. \quad (20)$$

This section introduces three examples of rate selection functions that account for uncertainty in the location estimate by selecting a conservative rate compared to the optimal rate selection function, i.e., $R_{\epsilon,i}(\hat{x}) < R_{\epsilon,i}^*(\hat{x})$. We limit the search to functions that satisfy the inequality constraint in (20) and then analyze the tradeoffs between reliability and throughput.

A. Backoff rate selection

The backoff rate selection function chooses the rate proportional to the ϵ -quantile for the MAR at the estimated location such that

$$R_{\epsilon,i}(\hat{x}) = k \cdot F^{-1}(\epsilon; \hat{x}, i), \quad (21)$$

where $0 < k \leq 1$ is the proportionality constant. The parameter k is interpreted as how conservatively the system selects the rate relative to the optimal rate selection when the location is perfectly known. Finding k such that the meta-probability achieves the target confidence δ requires knowledge of the system statistics, including location uncertainty, which may or may not be available in practice. For the sake of illustration, we simply perform a line search for $k \in (0, 1]$ and choose the maximum value such that the meta-probability meets the target confidence within a range of locations.

³This is equivalent to the statistical term *consistency* [15] where $R_{\epsilon,i}(\hat{x})$ converges in probability to $R_{\epsilon,i}^*(x)$ as $\text{Var}[\hat{x}] \rightarrow 0$.

B. Confidence intervals rate selection

This approach considers a confidence interval for estimated locations and then chooses the minimum rate within that interval. Denoting $\text{CI}_\alpha(\hat{x})$ as the confidence interval for x with confidence level $(1 - \alpha)$, the rate is selected as

$$R_{\epsilon,i}(\hat{x}) = \min_x \{F^{-1}(\epsilon; x, i) | x \in \text{CI}_\alpha(\hat{x})\}. \quad (22)$$

Setting an appropriate confidence level and obtaining the confidence interval again requires knowledge of the system statistics and similarly to the backoff method, we use a line-search to find the confidence level. Specifically, we use the approximate interval⁴

$$\text{CI}_\alpha(\hat{x}) = [\hat{x} - q_{1-\alpha/2}\sigma(\hat{x}), \hat{x} + q_{1-\alpha/2}\sigma(\hat{x})], \quad (23)$$

where q are the quantiles of the standard Gaussian distribution and $\sigma(\hat{x})$ is the standard deviation for localization at \hat{x} according to (10), which is assumed to be known.

C. Oracle rate selection

Lastly, *oracle rate selection* is introduced, which attempts to solve (20). This problem is solved by exhaustive search for the selected rate, which obviously requires a full statistical characterization of the system and is not of much practical interest. However, it serves as an upper bound and importantly shows that throughput suffers due to localization uncertainty even when the statistics of the system are fully known.

For the three aforementioned rate selection functions, the outage region in (16) is evaluated numerically. Interestingly, we observe that it reduces to a single interval for the considered 1D scenario, i.e., $S(x, i) = [x_{\min,i}, x_{\max,i}]$. Thus, according to the hierarchical model from (10), we can expand (17) as

$$\begin{aligned} P_{\hat{x}}(\hat{x} \in S(x, i)) &= \frac{1}{4\pi^2} \int_{[0, 2\pi]^2} P_{\hat{x}|\phi}(\hat{x} \in S(x, i) | \phi) d\phi \\ &= \frac{1}{4\pi^2} \int_{[0, 2\pi]^2} Q\left(\frac{x_{\min,i} - x}{\sigma(x; \phi)}\right) - Q\left(\frac{x_{\max,i} - x}{\sigma(x; \phi)}\right) d\phi, \end{aligned} \quad (24)$$

where Q is the tail distribution for a standard Gaussian variable.

V. EVALUATION OF RELIABILITY AND THROUGHPUT

Meta-probability in (15) and throughput ratio (19) are now evaluated under the different rate selection schemes from the previous section using the settings in Table I. The rate selection functions are calibrated to achieve a reliability of $\epsilon = 10^{-3}$ with confidence $\delta = 10^{-3}$ for $x \in [45, 955]$, and the results are depicted in Figs. 3 and 4 for the meta-probability and throughput ratio, respectively. Both (19) and (24) are evaluated through numerical integration.

Regarding Fig. 3, it is observed that for the backoff and confidence interval approaches; reliability generally is guaranteed with a higher probability the farther away from the BSs the UE is, which may seem counterintuitive. Two effects contribute to this: the decreasing location uncertainty and the

⁴The confidence interval in (23) is only approximate since it assumes that \hat{x} is Gaussian, where in reality, it is only conditionally Gaussian.

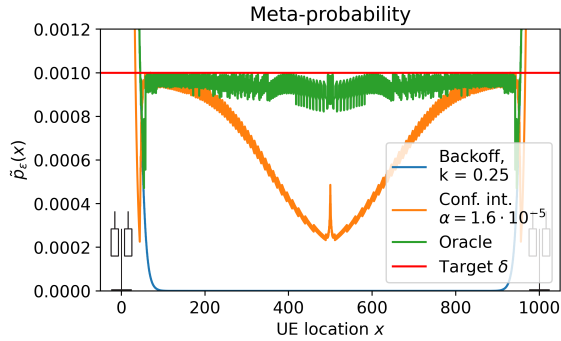


Fig. 3. Meta probability of the different rate selection schemes for each UE location $x \in [10, 990]$. Backoff rate selection uses $k = 0.25$ and confidence interval rate selection uses $\alpha = 1.6 \cdot 10^{-5}$.

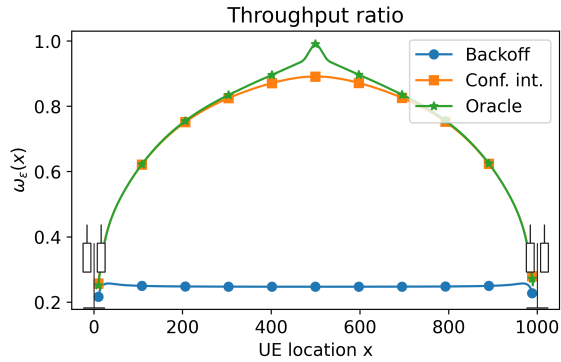


Fig. 4. Throughput ratio of the different rate selection schemes.

rapidly decreasing ϵ -quantile for R_{\max} as the distance between the UE and the BS increases (see Fig. 1). To understand the latter, note that the two methods select rates based on the ϵ -quantile. Therefore, even a small localization error close to a BS can cause the UE to pick a much higher rate, whereas the same error farther away causes a smaller change in the selected rate. In fact, considering that the changes in the average location uncertainty are almost negligible compared to the rapid variations in the ϵ -quantile (see Fig. 1), it is mainly the change in the quantile that causes the meta-probability to decrease, hence reliability to increase, with the distance to the BS⁵. For oracle rate selection, we see values close to the target confidence δ , as expected.

For Fig. 4, it is interesting to see that the throughput ratio for the backoff approach is more or less flat with $\omega_\epsilon(x) \approx k$. In contrast, the throughput ratios for the confidence interval and oracle approach have a strong dependence x . For these methods, we also observe that throughput increases farther away from the BSs, again explained by the ϵ -quantile for R_{\max} . To see this, consider the extreme case where the distribution $F(R; x, i)$ is constant for all locations x . Here, the UE would choose $R = F^{-1}(\epsilon; \hat{x}, i)$, which is invariant to the estimated location; thus, the meta-probability is zero, and the optimal throughput ratio is achieved. In our setup, when the UE is far away from the BSs, it experiences a similar case where the distribution is almost constant within the range of

⁵This has been numerically verified by computing the meta-probability under constant $\text{Var}[\hat{x}]$, where we see similar curves as in Fig. 3.

likely estimated locations (see Fig. 1), thus enabling the UE to be less conservative and achieve higher throughput. In summary, we observe degradation in the system when the UE is close to a BS and vice versa due to how quickly the ϵ -quantile for R_{\max} changes for different x , leading to the conclusion that lower but more spatially consistent channel statistics are desirable for location-based rate selection.

VI. CONCLUSIONS

This letter has analyzed the impact of location uncertainty on communication reliability through a rigorous statistical framework. Assuming a perfect (and known) mapping between location and channel statistics, we have shown that location uncertainty considerably impacts the reliability (characterized by the meta-probability of the outage event), especially as the user gets closer to the BSs. Conservative rate selection schemes can avoid this at the expense of a much lower throughput than the optimal one. Rapidly varying channel statistics in space have been shown to be particularly detrimental for the system. Different rate selection functions have been proposed, but ultimately this task requires accurate knowledge of channel statistics at different locations to ensure a certain level of reliability, and the resulting throughput can suffer when the rates are selected conservatively, compromising the usefulness of location as a rate selection proxy.

REFERENCES

- [1] A. Ghosh, A. Maeder, M. Baker, and D. Chandramouli, "5G evolution: A view on 5G cellular technology beyond 3GPP release 15," *IEEE Access*, vol. 7, pp. 127639–127651, 2019.
- [2] F. Maschietti, D. Gesbert, P. de Kerret, and H. Wymeersch, "Robust location-aided beam alignment in millimeter wave massive MIMO," in *GLOBECOM - 2017 IEEE Global Commun. Conf.*, pp. 1–6, 2017.
- [3] E. Dall'Anese, S.-J. Kim, and G. B. Giannakis, "Channel gain map tracking via distributed Kriging," *IEEE Trans. Veh. Technol.*, vol. 60, no. 3, pp. 1205–1211, 2011.
- [4] A. Azari, M. Ozger, and C. Cavdar, "Risk-aware resource allocation for urllc: Challenges and strategies with machine learning," *IEEE Commun. Mag.*, vol. 57, no. 3, pp. 42–48, 2019.
- [5] N. Barman, S. Valentin, and M. G. Martini, "Predicting link quality of wireless channel of vehicular users using street and coverage maps," in *IEEE 27th Annu. Int. Symp. Pers. Indoor Mobile Radio Commun. (PIMRC)*, pp. 1–6, 2016.
- [6] C. Studer, S. Medjkouh, E. Gonultaş, T. Goldstein, and O. Tirkkonen, "Channel charting: Locating users within the radio environment using channel state information," *IEEE Access*, vol. 6, pp. 47682–47698, 2018.
- [7] 3GPP, "Radio measurement collection for minimization of drive tests," Tech. Rep. 37.320, V 16.5.0, 3rd Generation Partnership Project, 06 2021.
- [8] M. Angelichinoski, K. F. Trillingsgaard, and P. Popovski, "A statistical learning approach to ultra-reliable low latency communication," *IEEE Trans. Commun.*, vol. 67, no. 7, pp. 5153–5166, 2019.
- [9] Y. Shen and M. Z. Win, "Fundamental limits of wideband localization—part i: A general framework," *IEEE Trans. Inf. Theory*, vol. 56, no. 10, pp. 4956–4980, 2010.
- [10] D. Tse and P. Viswanath, *Fundamentals of Wireless Communication*. Cambridge University Press, 2005.
- [11] H. Wymeersch and B. Denis, "Beyond 5G wireless localization with reconfigurable intelligent surfaces," in *2020 IEEE Int. Conf. Commun. (ICC)*, pp. 1–6, 2020. ISSN: 1938-1883.
- [12] E. Krouk and S. Semenov, *Modulation and Coding Techniques in Wireless Communications*. Wiley, 2011.
- [13] I. Guvenc and C.-C. Chong, "A survey on TOA based wireless localization and NLOS mitigation techniques," *IEEE Commun. Surveys Tuts.*, vol. 11, no. 3, pp. 107–124, 2009.
- [14] S. M. Kay, *Fundamentals of Statistical Signal Processing: estimation theory*. Prentice Hall signal processing series., Prentice-Hall, 1993.
- [15] H. Madsen and P. Thyregod, *Introduction to General and Generalized Linear Models*. CRC Press, 1 ed., 2011.